

# Discrete-space continuous-time models of marine mammal exposure to Navy sonar

CHARLOTTE M. JONES-TODD <sup>1,10</sup> ENRICO PIROTTA <sup>2,3,4</sup> JOHN W. DURBAN,<sup>5</sup> DIANE E. CLARIDGE,<sup>6</sup> ROBIN W. BAIRD,<sup>7</sup> ERIN A. FALCONE,<sup>8</sup> GREGORY S. SCHORR,<sup>8</sup> STEPHANIE WATWOOD,<sup>9</sup> AND LEN THOMAS<sup>4</sup>

<sup>1</sup>Department of Statistics, University of Auckland, Auckland 1142 New Zealand

<sup>2</sup>Department of Mathematics and Statistics, Washington State University, 14204 NE Salmon Creek Avenue, Vancouver, Washington 98686 USA

<sup>3</sup>School of Biological, Earth and Environmental Sciences, University College Cork, North Mall, Distillery Fields, Cork T23 N73K Ireland

<sup>4</sup>Centre for Research into Ecological and Environmental Modelling, The Observatory, University of St Andrews, St Andrews KY16 9LZ UK

<sup>5</sup>Southall Environmental Associates Inc., 9099 Soquel Drive, Suite 8, Aptos, California 95003 USA

<sup>6</sup>Bahamas Marine Mammal Research Organization, Marsh Harbour, Abaco, Bahamas

<sup>7</sup>Cascadia Research Collective, 218 1/2 W. 4th Avenue, Olympia, Washington 98501 USA

<sup>8</sup>Marine Ecology and Telemetry Research, 2420 Nellita Road NW, Seabeck, Washington 98380 USA

<sup>9</sup>Naval Undersea Warfare Center Division, Code 70T, Newport, Rhode Island 02841 USA

*Citation:* Jones-Todd, C. M., E. Pirotta, J. W. Durban, D. E. Claridge, R. W. Baird, E. A. Falcone, G. S. Schorr, S. Watwood, and L. Thomas. 2021. Discrete-space continuous-time models of marine mammal exposure to Navy sonar. *Ecological Applications* 00(00):e02475. 10.1002/eap.2475

**Abstract.** Assessing the patterns of wildlife attendance to specific areas is relevant across many fundamental and applied ecological studies, particularly when animals are at risk of being exposed to stressors within or outside the boundaries of those areas. Marine mammals are increasingly being exposed to human activities that may cause behavioral and physiological changes, including military exercises using active sonars. Assessment of the population-level consequences of anthropogenic disturbance requires robust and efficient tools to quantify the levels of aggregate exposure for individuals in a population over biologically relevant time frames. We propose a discrete-space, continuous-time approach to estimate individual transition rates across the boundaries of an area of interest, informed by telemetry data collected with uncertainty. The approach allows inferring the effect of stressors on transition rates, the progressive return to baseline movement patterns, and any difference among individuals. We apply the modeling framework to telemetry data from Blainville's beaked whale (*Mesoplodon densirostris*) tagged in the Bahamas at the Atlantic Undersea Test and Evaluation Center (AUTECE), an area used by the U.S. Navy for fleet readiness training. We show that transition rates changed as a result of exposure to sonar exercises in the area, reflecting an avoidance response. Our approach supports the assessment of the aggregate exposure of individuals to sonar and the resulting population-level consequences. The approach has potential applications across many applied and fundamental problems where telemetry data are used to characterize animal occurrence within specific areas.

**Key words:** aggregate exposure; area attendance; beaked whales; individual-level random effects; sonar disturbance; Template Model Builder; transition probability.

## INTRODUCTION

As a result of the expansion of human activities, individuals from wildlife populations are increasingly being exposed to a variety of anthropogenic stimuli (Sanderson et al. 2002, Halpern et al. 2008, Díaz et al. 2019). Some human activities can have nonlethal effects on exposed individuals, causing deviations in their natural patterns of behavior and physiology (Pirotta et al. 2018a, Frid

and Dill 2002). Current European Union (European Habitats Directive 92/43/EEC) and United States (Endangered Species Act, 16 U.S.C. §§ 1531 et seq.; Marine Mammal Protection Act, 16 U.S.C. §§ 1361 et seq.) legislation provides the basis for an assessment of the population-level consequences of these behavioral and physiological changes. Understanding where, when, and how often animals come into contact with human activities is the first step toward this assessment. In particular, quantifying population consequences requires an evaluation of (1) the proportion of the population that is exposed and (2) the aggregate exposure of each individual (i.e., the total duration and intensity of exposure to the stressor of interest during a biologically meaningful

Manuscript received 5 March 2020; revised 1 February 2021; accepted 19 May 2021; final version received 30 September 2021. Corresponding Editor: Stephen B. Baines.

<sup>10</sup>E-mail: c.jonestodd@auckland.ac.nz

period [Pirootta et al. 2018a]). Various factors influence the patterns of exposure of individuals in space and time. For example, a population's movement patterns (Jones et al. 2017, Pirootta et al. 2018b), the size of individual home ranges and the motivation underlying the use of the area of interest (e.g., whether the area contains foraging patches or is used solely for transit; Hückstädt et al. 2020) will all contribute to determine if each individual in a population is exposed at all and, if so, its aggregate exposure.

Many marine organisms rely on the use of sound for important life-history functions (e.g., communication and prey finding; Montgomery and Radford 2017). In recent decades, extensive work on the population consequences of disturbance has thus been motivated by growing concerns on the effects of increasing anthropogenic noise pollution in the ocean (Popper and Hawkins 2016), particularly on marine mammals (National Research Council 2005, Nowacek et al. 2007). Among the various sources of noise, cetacean populations may be affected by military operations using active sonar (Southall et al. 2016). Dedicated experiments and opportunistic exposure studies have shown that animals can respond to active sonars by changing their horizontal movement and diving behavior, leading to interruption of foraging activity, habitat displacement, and, potentially, changes in their physiology (Tyack et al. 2011, Southall et al. 2016, De-Ruiter et al. 2017, Falcone et al. 2017, Harris et al. 2018, Joyce et al. 2020). As such, current environmental impact statements conducted in the areas used for naval training activities (hereafter "ranges") require an assessment of the number of individuals that respond to sonar exercises; this number can be estimated from the probability of an individual getting exposed to the noise source, and the probability of responding when exposed to a certain noise level (Harris et al. 2018).

A suite of individual-based animal movement models has been developed to estimate the number of individuals that are exposed and respond over the duration of a single Navy exercise (Frankel et al. 2002, Houser 2006, Donovan et al. 2017, U.S. Department of the Navy 2018). However, these models are not suitable for the estimation of individuals' exposure to sonar over time and across multiple exercises, because their predictions become increasingly unrealistic when simulating movements for more than a few days, with individuals tending to diffuse away from the range area (Donovan et al. 2017). Moreover, simulating fine-scale animal movements over a long time period is computationally intensive, and unnecessary when the animals are outside the area of interest. To overcome these difficulties, most existing models treat each day independently and do not tally the number of times individuals are exposed over longer periods, even though predictions of population-level effects may change drastically depending on the level of aggregate exposure (Donovan et al. 2017, Pirootta et al. 2018a). An alternative method is required to

characterize the long-term patterns of individual occurrence in the target area and the effect of exposure and response to disturbance on these patterns. Such a method would then form the basis for a detailed quantification of the number of times each individual is exposed when inside the area and thus susceptible to respond to disturbance. In order to capture the various aspects of the ecology of a population that could influence usage of the area, the method should be informed using empirical movement data collected from individuals in the population over a comparable time scale. Modern satellite telemetry technologies allow us to track marine mammal movements for long periods, and could therefore be used to characterize the attendance to specific areas of interest. However, they are often associated with substantial spatial error in animal relocations (Costa et al. 2010).

In this study, we develop a discrete-space, continuous-time analytical approach to monitor the occurrence of animals in an area of interest and their transition rates across the boundaries of that area, informed by telemetry data collected with uncertainty. Our goal is to be able to estimate the aggregate exposure and response to sonar of individuals in a population over biologically relevant time periods. The approach allows for differences in movement patterns among individuals. Importantly, the potential repulsive effect that the activity under analysis has on the animals and the progressive decay of such effect over time can also be quantified (Tyack et al. 2011, Moretti et al. 2014). While the approach is motivated by and applied to case studies involving the exposure of cetaceans to disturbance from active sonar operations on U.S. Navy ranges, it is widely applicable to other contexts and types of stressors. The method would also be useful in situations where the estimation of the movements in and out of an area is of interest, irrespective of the presence of anthropogenic stressors (e.g., to monitor the attendance of individuals to a protected area).

## MATERIALS AND METHODS

### *Telemetry data and exposure information*

We use satellite telemetry data from seven Blainville's beaked whales (*Mesoplodon densirostris*) tagged between 2009 and 2015 within or near the Atlantic Undersea Test and Evaluation Center (AUTECE), in the Bahamas (Fig. 1). This region is regularly used by the U.S. Navy to carry out military exercises with active sonar. Tagging was carried out in advance of large-scale exercises (Submarine Command Courses) to monitor resulting changes in the animals' movement behavior.

Data collection techniques are described in detail in Joyce et al. (2020). Animals were fitted with Wildlife Computers SPLASH transmitters ( $n = 2$ , Mk-10; Wildlife Computers, Redmond, Washington, USA) and SPOT model tags ( $n = 5$ , AM-S240A-C; Wildlife

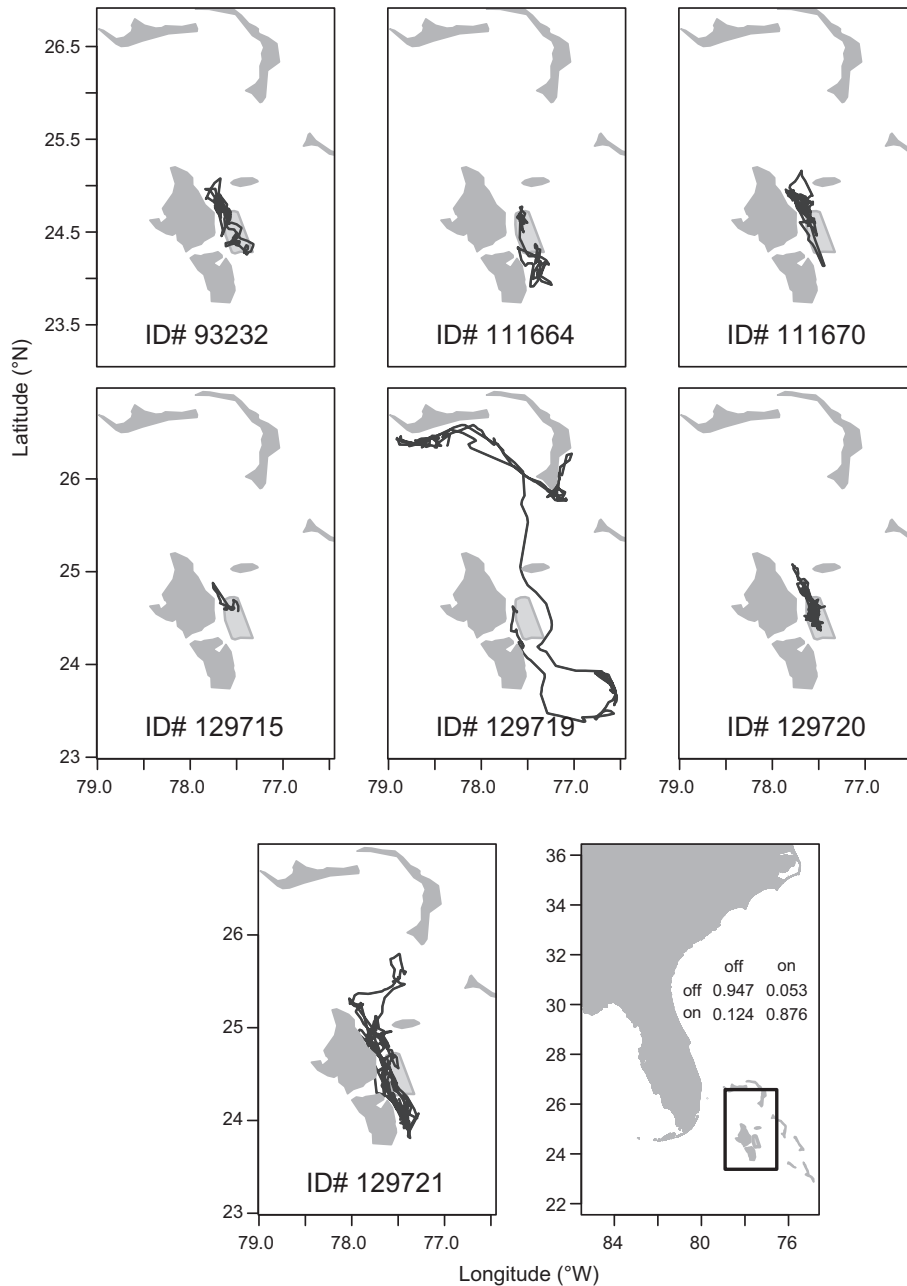


FIG. 1. Estimated tracks of the seven Blainville's beaked whales (*Mesoplodon densirostris*), at the AUTECH range (shown by the light gray polygon), Bahamas. The bottom right plot shows the plotted region, for each individual, in relation to Florida, USA; the calculated raw transition probability matrix for sequential transitions across AUTECH range boundaries, averaged across individuals, is shown as an inset table. The raw ARGOS data can be seen in Appendix S1: Fig. S1.

Computers) in the Low Impact Minimally Percutaneous External-electronics Transmitter (LIMPET) configuration; see Appendix S1: Table S1. Tags were attached on or near the dorsal fin from distances of 5–25 m using a crossbow or black powder gun (Tyack et al. 2011, Joyce et al. 2020). Location estimates of tagged whales were provided by the Argos system based on the Kalman filtering method (Lopez et al. 2013). Tags were scheduled

to transmit up to 700 times during 12–18 h of each day, timed to coincide with passes of satellites from the Argos satellite system.

Information on the use of mid-frequency active sonars (MFAS) at AUTECH was available from records in the U.S. Navy's internal Sonar Positional Reporting System (SPORTS) database (including, but not limited to, the Submarine Command Courses analyzed in Joyce et al.

[2020]). While SPORTS data are known to suffer from transcription errors and incomplete records, they offered the best available source of sonar information. Specifically, we extracted bouts of high-power (hull-mounted, surface-ship) and mid-power (helicopter-deployed) MFAS use (sensu Falcone et al. [2017]) during tag deployment periods, and calculated the number of days since exposure to a sonar event for each individual relocation. The outline of the hydrophone array at AUTECH was used as the range boundary, and, for simplicity, animals were considered exposed when occurring within this area during sonar activity.

In addition to tracks of *M. densirostris* from AUTECH, we applied our modeling approach to four other cetacean species with varying movement behavior and ecology, occurring over two different U.S. Navy ranges, the Hawai'i Range Complex (HRC) and the Southern California Range Complex (SOCAL). Details of these additional case studies and the challenges they present for estimating the effects of sonar exposure are described in Appendix S2.

#### Overview of modeling approach

We model movement probability into and out of a region encompassing a Navy range where sonar exercises take place, and how this probability is influenced by the use of sonar on the range. The models presented below are implemented in the `mmre` R package; see the package ([available online](#)) and Appendix S3 for further details and examples.<sup>11</sup>

Our modeling approach consisted of three interconnected steps. First, raw tracking data were filtered for obvious mistakes in animal relocation, identified by unrealistic horizontal displacement. While subsequent models can accommodate uncertainty in satellite-derived locations of the animals, aberrant observations can negatively affect model performance (Patterson et al. 2010). We therefore filtered recorded Argos locations using the R package `argosfilter` (Freitas 2012), so that highly unlikely observations (i.e., those implying a horizontal displacement >15 m/s) were removed. Second, filtered tracks were adjusted for Argos location uncertainty using a continuous-time correlated random walk state-space model, which returned estimated tracks based on the underlying movement model (*Continuous-time correlated random walk*). Finally, estimated tracks were analyzed using a discrete-space continuous-time Markov model that quantified the transition rates across range boundaries and the effect of exposure to sonar disturbance on animal movement patterns (*Discrete-space continuous-time Markov model*).

Our approach is conceptually comparable to the continuous-time Markov chain model proposed by Hanks et al. (2015). The authors discretize space into a grid, and use tracking data to model residence time in

each occupied cell and transitions to neighboring cells in a Generalized Linear Modeling framework. Recently, a discrete-space continuous-time model has been developed to analyze whale diving behavior from time series of binned depth observations (Hewitt et al. 2021). Here, we reduce gridded space to two larger areas: on and off a Navy range. Occurrence within each area is used to determine the known states of an individual at the observation times, which are then analyzed in a multi-state modeling framework in continuous time to infer instantaneous transition rates (Jackson 2011). Our aim is to assess the patterns of attendance to an area of interest (as a function of exposure to a stressor), as opposed to the role of environmental variables on individuals' movement decisions. Similarly to Hooten et al. (2016) and Buderman et al. (2018), we extend the model to include individual random effects on the transition rates, thus making the model hierarchical. Because individual Argos locations are provided with error, we first impute the tracks using a continuous-time correlated random walk (Johnson et al. 2008, Albertsen et al. 2015), as in Hanks et al. (2015). In line with their work, we also propose multiple imputation to fully propagate the uncertainty associated with estimated tracks to the results of the Markov model (*Discrete-space continuous-time Markov model*). In contrast with the formulation of Hanks et al. (2015) or Jackson (2011), our approach is fitted using Template Model Builder (TMB; Kristensen et al. 2016), which implements automatic differentiation and applied Laplace approximation to complex random-effect models.

#### Continuous-time correlated random walk

Due to the uncertainty associated with Argos locations, individual tracks were estimated using the continuous-time correlated random walk model (CTCRW) described in Johnson et al. (2008) and Albertsen et al. (2015) using the R package `argosTrack` (Albertsen 2017).

In brief, the CTCRW model is a state-space model (SSM) with measurement equation given by  $y_{ct} = \mu_{ct} + \varepsilon_{ct}$  where  $y_{ct}$  is the  $c$ th coordinate ( $c = 1$  [longitude],  $2$  [latitude]) of the observed location of an animal at time  $t$  ( $t = 1, 2, \dots, n$ ) with measurement error term  $\varepsilon_{ct}$ . As in Albertsen et al. (2015) the joint distribution of  $\varepsilon_{1t}$  and  $\varepsilon_{2t}$  is a bivariate  $t$  distribution. The term  $\mu_{ct}$  is then the "true"  $c$ th coordinate location of the animal at time  $t$ . This location process,  $\mu_{ct}$ , is obtained by integrating over the assumed instantaneous velocity of the animal at time  $t$ . This velocity is assumed to follow an Orstein-Uhlenbeck (OU) process (see Albertsen et al. [2015] for further details).

#### Discrete-space continuous-time Markov model

Continuous-time Markov models describe how an individual transitions between states in continuous time. Given that an individual is in state  $S(t)$  at time  $t$ , the transition intensity,  $q_{rs}(t, z(t))$ , represents the immediate

<sup>11</sup> <https://github.com/cmjt/mmre>

hazard of moving from one state  $r$  to another state  $s$ , and may be dependent on the time  $t$  of the process as well as some time-varying covariate  $z(t)$ . These transition intensities can be written as

$$q_{rs}(t, z(t)) = \lim_{\delta t \rightarrow 0} \mathbb{P}(S(t + \delta t) = s | S(t) = r) / \delta t \quad (1)$$

and form a square matrix  $\mathbf{Q}$  with elements  $q_{rs}$  where  $q_{rr} = -\sum_{s \neq r} q_{rs}$  (i.e., the rows of  $\mathbf{Q}$  sum to zero) and  $q_{rs} \geq 0$  for  $r \neq s$ .

Here, the state at observation time  $t$  is determined by where the animal is located, i.e.,  $\mu_{ci}$  (see *Continuous-time correlated random walk*). We consider only two states (i.e.,  $r, s = \{1, 2\}$ ) where state 1 = off-range (i.e., outside the area used by the Navy for military operations) and state 2 = on-range (i.e., inside this area, see Fig. 1).

The equation of our model is given by

$$\log(q_{k,rs}(z_k(t))) = (\beta_{0,rs} + u_{k,rs}) + \beta_{1,rs} \exp(-\beta_{2,rs} z_k(t)) + \eta \quad (2)$$

where  $\beta_{0,rs}$  is the intercept term, representing baseline transition rates (on the log-scale), and  $u_{k,rs}$  indicates the individual-level random effects (for individual  $k = 1, \dots, 7$ ) on the transition rates. Each  $u_k = \{u_{k,rs}, u_{k,rs}\}$  follows a zero-mean bivariate Gaussian distribution (between states  $r$  and  $s$ ) with  $2 \times 2$  variance covariance matrix  $\text{diag}(\sigma_u^2, \sigma_u^2)$ . The time-varying covariate is given by

$$z_k(t) \begin{cases} = 0 & \text{during exposure} \\ > 0 & \text{otherwise} \end{cases}$$

and represents the number of days since an individual was exposed to a sonar event. The Gaussian random error term is represented by  $\eta$ .

Here,  $\beta_{1,rs}$  represents the change in transition rate, on the log scale, during exposure (i.e.,  $z_k(t) = 0$  thus  $\exp(-\beta_{2,rs} z_k(t)) = 1$ ). We constrain  $\beta_{2,rs} \geq 0$  for all  $r \neq s$ ; by doing so, as the number of days since an individual was exposed to sonar,  $z_k(t)$ , increases, transition rates decay exponentially toward their baseline values,  $\beta_{0,rs}$  (on the log scale). Therefore,  $\beta_{2,rs}$  for  $r \neq s$  can be thought of as the lessening effect of sonar exposure on the transition rates after the termination of sonar. It should be noted that, while we were limited by sample size in our case, individual differences in the animals' response to sonar could also be investigated, e.g., by including a random effect on the  $\beta_{1,rs}$  and  $\beta_{2,rs}$  parameters. Parameter estimates are obtained via minimization of the negative log-likelihood,  $-\log(L(\mathbf{Q}))$ ; see Appendix S4 for details.

We use a likelihood ratio test (LRT) and Akaike Information Criterion (AIC) to compare the full model in Eq. 2 with two reduced versions: (a) a null model that only includes baseline transition rates and (b) a model with individual random effects

(but no effect of exposure). We refer to the full model as (c). The test statistic for the LRT,  $\lambda_{LR} = -2(\log(L(\mathbf{Q})_0) - \log(L(\mathbf{Q})_A))$  (i.e., twice the difference between the log-likelihoods of the reduced, subscript 0, and alternative, subscript A, models), follows a  $\chi^2$  distribution with degrees of freedom equal to the difference in the number of estimated parameters in each model. We quantify the number of random-effect parameters as  $14 + 1 = 15$  (i.e.,  $2 \times 7 = 14$  for the individual-level random effect means, twice the number of individuals, and 1 for the bivariate Gaussian variances, fixed to be equal). We calculate the number of parameters in each model as the sum of the random-effect and the fixed-effect parameters. Using AIC for models that include random effects depends on the intended level of inference and should be carried out with caution as the penalty is not obvious (Vaida and Blanchard 2005, Bolker et al. 2009). Here, we are interested in population-level inference and therefore follow the recommendation of Vaida and Blanchard (2005) to use the marginal AIC for model comparison.

We used a multiple imputation procedure to show how the uncertainty associated with the Argos tracks could be propagated to the Markov model (Hanks et al. 2015, Scharf et al. 2016, 2017, Buderman et al. 2018). For each of the seven individuals, a total of 100 tracks were imputed using the estimated bivariate  $t$  distribution of measurement error from the CTCRW model, fitted to the Argos tracks (see *Continuous-time correlated random walk*). We fitted the model given by Eq. 2 to the 100 imputed data sets (each containing one potential track per individual), and calculated the pooled point estimate and variance of each parameter as in McClintock (2017).

### Simulation

To assess the performance of the proposed model, we used the estimated parameter values from the fitted model (Eq. 2) to simulate new data sets. Specifically, we simulated the states of individuals at each observed time using the fitted transition probabilities. This was done 500 times for each individual. We refitted the model to the 500 simulated data sets, and calculated root mean squared errors for each parameter, as well as the percentage errors for  $\beta_{1,12}$ ,  $\beta_{1,21}$ ,  $\beta_{2,12}$ , and  $\beta_{2,21}$  (that is, the parameters relating to the sonar effect).

### Goodness of fit

To assess the goodness of fit of the Markov model, we took a similar approach to Aguirre-Hernández and Farewell (2002). Specifically, we partitioned observations from each individual by time and covariate value (time since exposure), and compared the observed number of transitions,  $o$ , to the number of transitions expected under the fitted model,  $e$ . Bins were created by splitting the data into quantiles, [0–25%], [25–50%],

[50–75%], and [75–100%], based on observation times and covariate values (using estimated transition rates as recommended by Aguirre-Hernández and Farewell [2002]). The expected number of transitions in each time and covariate bin were calculated as the sum of the estimated probabilities classified in that category.

We carried out a Pearson-type goodness-of-fit test similar to that proposed by Aguirre-Hernández and Farewell (2002) using the test statistic  $T = \sum_{uhk} \left( (o_{uhk} - e_{uhk})^2 / e_{uhk} \right)$ , where  $u$  represented the number of levels defined by the quantiles of the observation times,  $h$  represented the groupings due to the covariate, and  $k$  was the individual whale. We assumed a chi-squared distribution for this test statistic and used both a liberal and a conservative number of degrees of freedom; these were calculated as (1) the minimum number of independent bins ( $7 \times 4 \times 3 \times 2 = k \times u \times h \times n_{states}$ ) and (2) the minimum number of independent bins minus the number of estimated parameters,  $n_p = 21$ , respectively.

RESULTS

Following the first two steps of our analytical approach, we obtained estimated tracks for the seven Blainville’s beaked whales (Fig. 1). Note that, while all adult individuals remained in proximity of the Navy range, the only tagged subadult engaged in a wide-ranging trip across the region. The discrete-space continuous-time Markov model was then used to estimate the transition rates across the AUTEK range boundaries (Table 1). Differences in baseline transition rates among individuals were captured by the inclusion of individual-level random effects; Figs. 2 and 3 show that there was noteworthy variation among whales. Appendix S1: Fig. S2 shows the estimated individual-level random effects.

Comparing models (b) and (a),  $\lambda_{LR} = 27.22$  and, under  $\lambda_{LR} \sim \chi^2_{15}$ ,  $P(\lambda_{LR} > 27.22) = 0.02$ , suggesting that the individual-level random effects should be retained. Comparing models (c) and (a),  $\lambda_{LR} = 41.56$  and, under  $\lambda_{LR} \sim \chi^2_{19}$ ,  $P(\lambda_{LR} > 41.56) = 0.006$ , suggesting that the decaying effect of exposure should be retained in the model. Using the marginal AIC (Vaida and Blanchard 2005) also confirmed the results of the LRT (Table 1).

Using the model given by Eq. 2, we detected a change in transition rates following exposure to sonar activities (Table 1). The estimated  $\hat{\beta}_1 = \{\hat{\beta}_{1,12}, \hat{\beta}_{1,21}\}^T$  parameters represent the effect on the log rate of transition off-on and on-off the range, respectively, during the time an individual was exposed to sonar. During exposure (i.e.,  $z(t) = 0$  in Eq. 2), transitions onto the range (off-on) decreased ( $\hat{\beta}_{1,12} = -0.60$ ) and transitions off the range (on-off) increased ( $\hat{\beta}_{1,21} = 1.75$ ). The increase in on-off transitions during sonar exposure is illustrated in Fig. 3, where sonar activity is indicated by vertical gray lines.

The  $\hat{\beta}_2 = \{\hat{\beta}_{2,12}, \hat{\beta}_{2,21}\}^T = \{0.78, 0.85\}$  parameters describe the exponential decay to the baseline transition rates off-on range and on-off range, respectively. Figs. 2 and 3 illustrate this exponential decay for each individual; the effect of sonar exposure on the transition rates was estimated to end approximately 3 d after the activity ended (i.e., when transition probabilities returned to their baseline values).

Refitting the Markov model to 500 simulated data sets, generated using the estimates in Table 1, suggested that the model was able to retrieve the values of the parameters with limited bias. The root mean squared error (RMSE) and bias for each parameter in the simulation study are given in Appendix S1: Table S6, while the percent errors for the parameters relating to sonar effect are shown in Appendix S1: Fig. S4.

TABLE 1. Table of estimated parameters, log-likelihood, and Akaike information criterion (AIC) values for the fitted models; standard errors are given in brackets.

Model, $n_p$	Random/exposure	$P(t = 1)^\dagger$	log-likelihood	AIC	$\hat{\beta}_0$	$\hat{\beta}_1$	$\hat{\beta}_2$	Time to fit (s)
(a), 2	-/-	$\begin{bmatrix} 0.877 & 0.123 \\ 0.505 & 0.495 \end{bmatrix}$	-257.04	518.08	$\begin{bmatrix} -1.65 & (0.18) \\ -0.23 & (0.16) \end{bmatrix}$	-	-	0.664
(b), 17	+/-	$\begin{bmatrix} 0.858 & 0.142 \\ 0.525 & 0.475 \end{bmatrix}$	-243.43	492.87	$\begin{bmatrix} -1.45 & (0.40) \\ -0.14 & (0.40) \end{bmatrix}$	-	-	251.8
(c), 21	+/+	$\begin{bmatrix} 0.807 & 0.193 \\ 0.421 & 0.579 \end{bmatrix}$	-236.26	486.51	$\begin{bmatrix} -1.21 & (0.48) \\ -0.43 & (0.47) \end{bmatrix}$	$\begin{bmatrix} -0.60 & (0.61) \\ 1.75 & (0.56) \end{bmatrix}$	$\begin{bmatrix} 0.78 & (1.01) \\ 0.85 & (0.60) \end{bmatrix}$	925.7

Notes: The first column gives the model name as discussed in *Discrete-space continuous-time Markov model* and the associated number of parameters,  $n_p$ . The second column indicates whether the model includes individual random effects (random) or an exposure component (exposure). For example, +/- indicates that a model includes both components. The baseline transition rates, on the log scale, are given by  $\hat{\beta}_0 = \{\hat{\beta}_{0,12}, \hat{\beta}_{0,21}\}^T$ . Where applicable, the changes in transition rate during exposure are given by  $\hat{\beta}_1 = \{\hat{\beta}_{1,12}, \hat{\beta}_{1,21}\}^T$  and the decay parameters are given by  $\hat{\beta}_2 = \{\hat{\beta}_{2,12}, \hat{\beta}_{2,21}\}^T$ . The final column gives the time taken, in seconds, to fit each model using system.time() in R 4.0.2 on a laptop computer with a 2.5 GHz processor. Here, † denotes that  $P(t = 1)$  is calculated at the baseline transition rate (i.e., ignoring any other effects, if there are any).

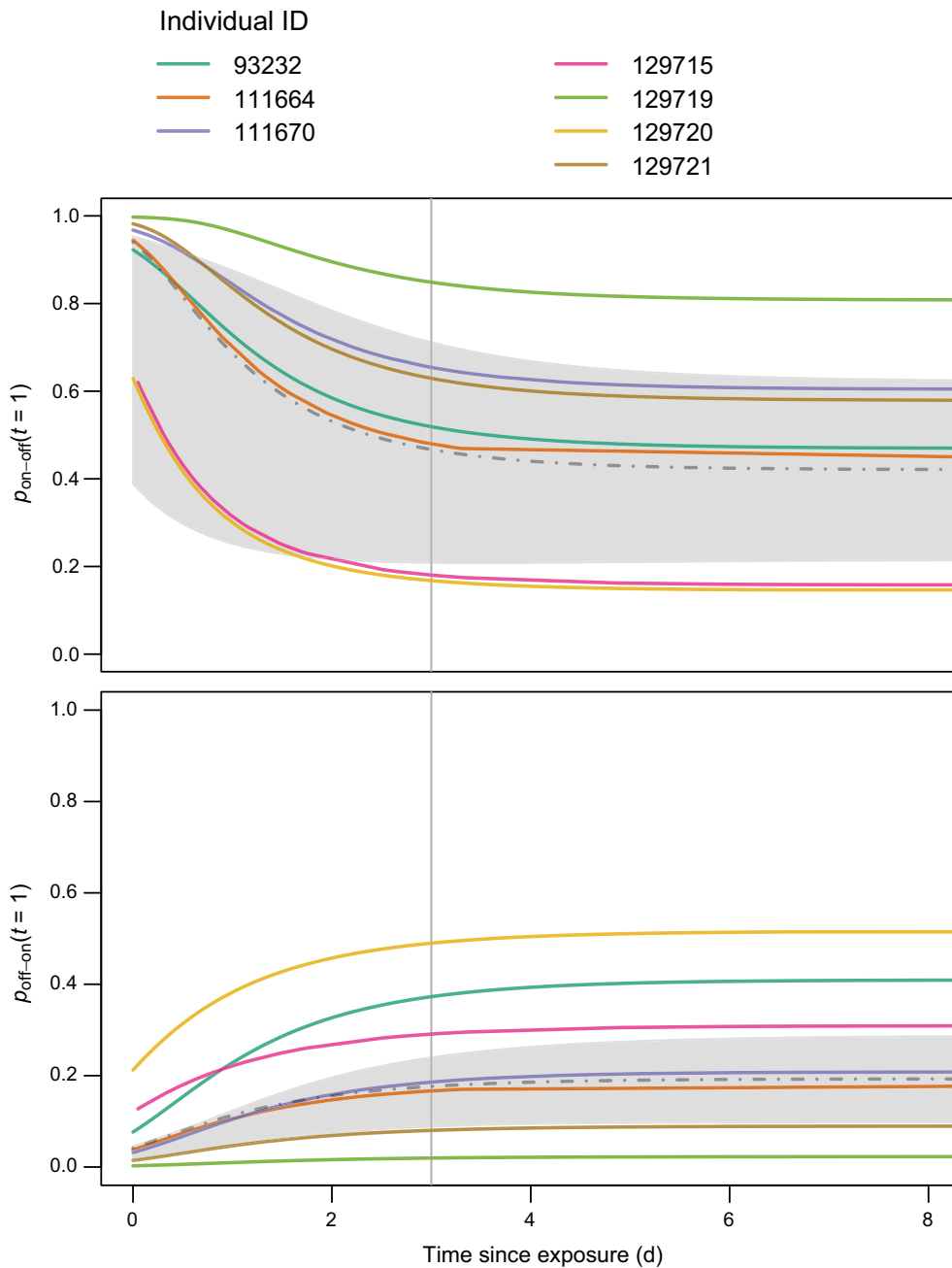


FIG. 2. Estimated transition probabilities for each of the seven Blainville's beaked whales as a function of time since exposure to sonar, calculated at 1 d since tagging ( $t = 1$ ); the corresponding transition rate is given by Eq. 2. In each plot, colors indicate different individuals; the top plot shows on-off transition probabilities and the bottom plot shows off-on transition probabilities. The gray-shaded areas show the 95% confidence interval around the mean transition probabilities (dashed gray lines) as a function of time since exposure. The vertical line indicates 3 d since exposure.

The multiple imputation procedure allowed us to successfully propagate the uncertainty in the telemetry tracks across all modeling steps. A subset of 20 imputed tracks obtained using the parameter values from the fitted CTCRW model is shown in Appendix S1: Fig. S3 for three individuals. Uncertainty in the exact locations

of the individuals had little effect on the estimated transition rates, as suggested by the parameter values averaged across the 100 fitted models (Table 2 and Appendix S1: Fig. S4).

The comparison of observed transitions,  $o$ , with those expected,  $e$ , for each individual  $k$  (see *Goodness of fit*)

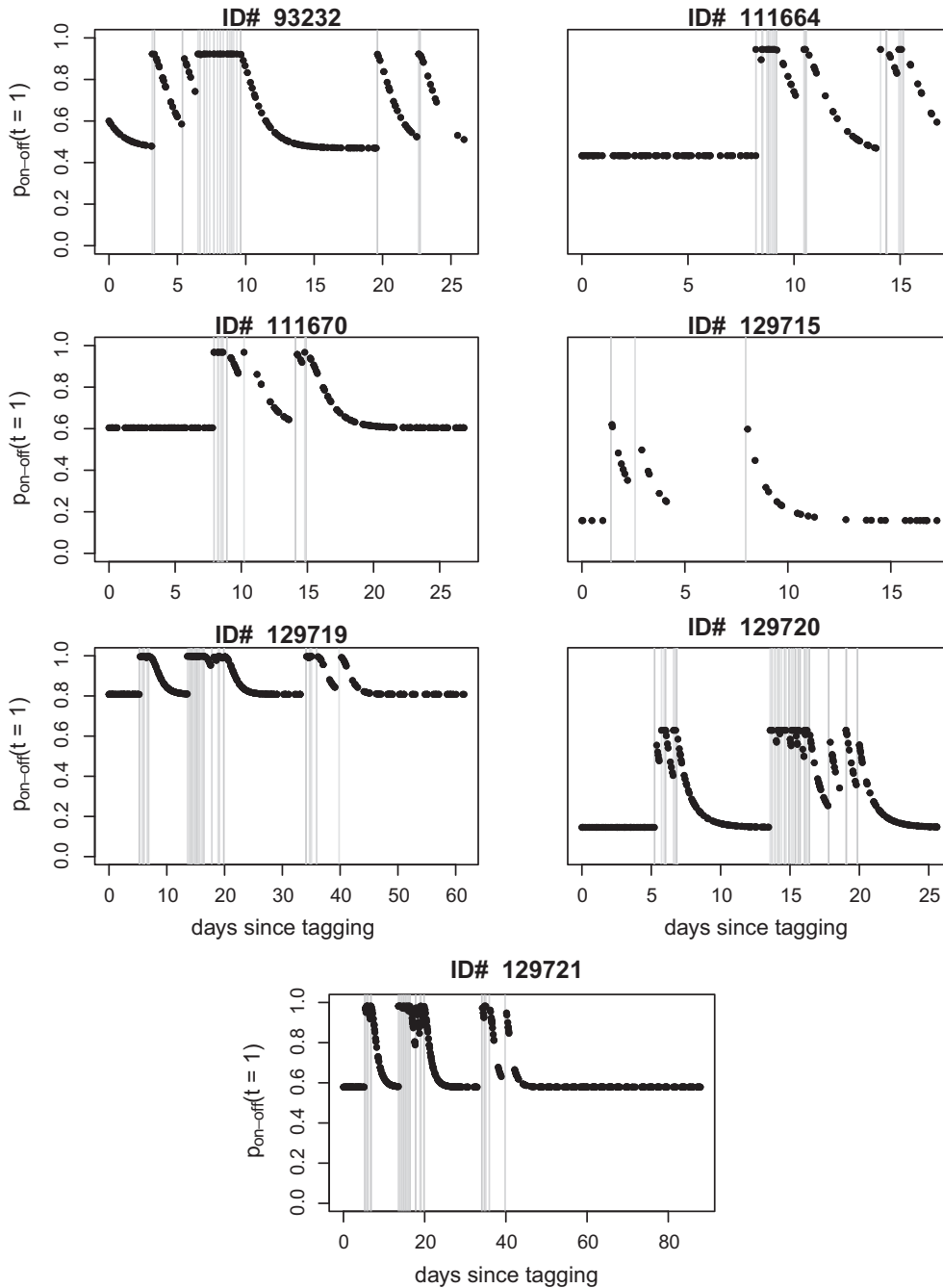


FIG. 3. Fitted on-off range transition probabilities,  $p_{21}(t = 1)$ , for each of the seven Blainville's beaked whales (derived from the corresponding transition rates given by Eq. 2). In each plot, the vertical gray lines indicate the time of sonar events; the points represent the time of observed locations (in days) of each individual since tagging. The different horizontal asymptotes in each panel illustrate the differences in baseline transition rates among individuals.

suggested that the goodness-of-fit of the Markov model was satisfactory Appendix S1: Fig. S4c. The Pearson-type test returned a test statistic  $T = 168.44$ ; under  $T \sim \chi^2_{147}$ ,  $P(T > 168.44) = 0.109$ , and under  $T \sim \chi^2_{168}$ ,  $P(T > 168.44) = 0.476$ , i.e., we have no evidence to suggest that observed frequencies in each bin are significantly different from those estimated by our model.

#### DISCUSSION

We developed a modeling approach that quantifies the rates at which animals move across the boundaries of a discrete area of interest. The model can therefore be used to describe patterns of attendance to that area. Individual differences in movement and ranging behavior,



TABLE 2. For each of the seven Blainville's beaked whales, 100 sets of continuous-time correlated random walk (CTCRW) tracks were imputed and the fitted model given by Eq. 2.

	$P(t = 1)^\dagger$	$\hat{\beta}_0$	$\hat{\beta}_1$	$\hat{\beta}_2$
Est. (Var.)	$\begin{bmatrix} 0.801 & 0.199 \\ 0.416 & 0.584 \end{bmatrix}$	$\begin{bmatrix} -1.18 & (0.41) \\ -0.44 & (0.24) \end{bmatrix}$	$\begin{bmatrix} -0.61 & (3.59) \\ 0.64 & (8.92) \end{bmatrix}$	$\begin{bmatrix} 1.97 & (0.59) \\ 0.98 & (0.52) \end{bmatrix}$

Notes: The table shows the pooled point estimate (Est.) and variance (Var.) of each parameter, calculated following McClintock (2017). As in Table 1,  $\dagger$  denotes that  $P(t = 1)$  is calculated at the baseline transition rate.

which may lead to heterogeneity in area use, are explicitly evaluated. By fitting a movement model to the raw telemetry tracks, uncertainty in animal relocations can also be accounted for. Moreover, because the Markovian component is formulated in continuous time, the approach does not require observations regularly sampled in time. These features are important, because wildlife telemetry often involves irregular relocations with substantial measurement error (Patterson et al. 2017). Crucially, the method we propose can be used to investigate the repulsive (or attractive) effect of a given stressor or activity, operating either within or outside the target area and affecting the propensity of an individual to cross the boundaries in either direction. Our simulation exercise showed that the model performs well at estimating transition rates and any change associated with exposure to disturbance.

We used a CTCRW model to account for uncertainty in animal relocations (Johnson et al. 2008, Albertsen et al. 2015). Alternative movement models could be fitted, depending on the sampling frequency and degree of measurement error in the telemetry data (Patterson et al. 2017). Irrespective of the underlying movement model, we showed how a multiple imputation procedure can be used to propagate any such uncertainty (Hanks et al. 2015, Scharf et al. 2016, 2017, Buderman et al. 2018). Our results suggest that location error does not alter the conclusions here, probably due to the size of the target area in relation to the estimated uncertainty. In situations where the area of interest is smaller, particularly with respect to the measurement error associated with telemetry locations, occurrence inside the area (i.e., an animal's state) could become uncertain, warranting the extension of the approach to a hidden Markov model (Langrock et al. 2012).

In this study, we applied the proposed approach to a specific management problem: the assessment of the effects of exposure to military sonar operations within navy ranges on the movement behavior of cetaceans, and the resulting attendance of individuals to these range areas (Nowacek et al. 2007, Southall et al. 2016, Bernaldo de Quirós et al. 2019). When fitted to tracking data from Blainville's beaked whales tagged on or near the AUTECH U.S. Navy range in the Bahamas, the model detected a change in the animals' movements following exposure. Individual whales that were on the range at the time of exposure showed an increased tendency of

leaving the range, while individuals that were outside the range area had a lower propensity to move onto the range, overall indicating an avoidance response to sonar. This effect was found to last for approximately three days after the end of the exposure, during which the transition rates progressively returned to their baseline values.

The implications of these results are twofold. First, they contribute to the increasing body of evidence suggesting that military sonar operations can cause changes in the behavior of exposed beaked whales (Tyack et al. 2011, De-Ruiter 2013, Stimpert et al. 2014, Manzano-Roth et al. 2016, Falcone et al. 2017, Harris et al. 2018, Bernaldo de Quirós et al. 2019, Wensveen et al. 2019). Dedicated experimental studies, as well as observational studies, have shown that these species modify their horizontal movement and diving pattern when exposed to simulated or real sonar in this and other areas (McCarthy et al. 2011, Tyack et al. 2011). In particular, passive acoustic monitoring of whale echolocation clicks has previously suggested that Blainville's beaked whale detections decline within the range area in AUTECH during sonar exercises, returning to baseline levels after approximately three days. Using the same telemetry data we have analyzed here, and focusing only on the effects of large-scale exercises (Submarine Command Courses), a recent study has provided further indication that this indeed corresponds to animals moving out of the range, rather than cessation of acoustic vocalizations (Joyce et al. 2020). With the proposed approach, we were able to quantify this tendency in terms of individual transition rates, and show that avoidance emerges in response to all sonar exercises occurring on the range. It has been suggested that human disturbance is perceived by wildlife as a form of predation risk, and, as such, can elicit comparable reactions, for example attempts to move away from the stressor (Frid and Dill 2002). A similar response could also arise indirectly if beaked whale prey became less available due to sonar activity (e.g., through displacement or changes in patch characteristics). We detected this behavioral change despite the regular exposure of this population to sonar disturbance in the range area, which poses interesting questions on the role of tolerance, habituation, and availability of alternative habitat (Harris et al. 2018).

Secondly, our model can support the assessment of an individual's aggregate exposure to a stressor (that is, the

total duration and intensity of exposure), which is required to evaluate the consequences of disturbance on individual fitness and, ultimately, population dynamics (Pirotta et al. 2018a). In particular, the model estimates the patterns of occurrence of an individual in the area where the stressor operates, which can then be combined with approaches that simulate fine-scale movements. To date, these simulations have incurred the problem that, as time progresses, simulated individuals tend to drift away from the target area (Frankel et al. 2002, Houser 2006, Donovan et al. 2017), leading to unrealistic movement patterns and thus compromising the ability to estimate aggregate exposure over time scales that are biologically relevant (e.g., 1 yr). The results of our model can inform realistic simulations of the occurrence in the area where an individual is potentially exposed, and ignore the behavior when outside such area (although this may require adjusting the range boundaries to account for noise propagation and potential exposure outside the instrumented area (Joyce et al. 2020), similarly to the other case studies in Appendix S2). In practice, the estimated transition probabilities could be used to simulate the daily presence or absence of an individual inside the area where it is susceptible to exposure; when present, finer-scale approaches could be used to model its interactions with the stressor inside the area. In some cases (e.g., when animals do not show high residency levels), this will also save substantial computation time, which is important when many scenarios of disturbance need to be simulated efficiently for large populations.

Model results highlighted differences among individuals in transition rates and presence on the range, which will result in heterogeneous levels of aggregate exposure within the population (Jones et al. 2017, Pirotta et al. 2018b). Differences among individuals could be explained by sex (Stewart 1997), age (Carter et al. 2020), life history stage (Ersts and Rosenbaum 2003, Pack et al. 2017), body condition (Chaise et al. 2018), exposure history (Bejder et al. 2006), or social preferences (Ersts and Rosenbaum 2003, Hauser et al. 2007). This information, when available, could readily be incorporated into the model as fixed effects on the transition rates. These differences are relevant because long-term effects on individual vital rates tend to emerge from the chronic disruption of activity budget and the impaired ability to acquire energy (Pirotta et al. 2018a). Therefore, characterizing variation in exposure and identifying the proportion of the population with high exposure level will ultimately contribute to the assessment of the population-level consequences of disturbance resulting from human activities, an important target for many regulatory frameworks (National Research Council 2005, Pirotta et al. 2018a).

The application of the modeling approach to other case studies in different U.S. Navy ranges demonstrates some of the outstanding challenges associated with this analysis (see Appendix S2). The model might not be appropriate in situations where the animals rarely leave

the target area, as shown for rough-toothed dolphins *Steno bredanensis* in Hawai'i (Baird 2016, Baird et al. 2019) and Cuvier's beaked whales *Ziphius cavirostris* in southern California (Falcone et al. 2017). In the latter case, the short time scale of documented behavioral responses (Falcone et al. 2017) compared to the resolution of the telemetry data further complicates the use of the model. In that region, the model could be more appropriate for fin whales *Balaenoptera physalus*, which regularly transits in and out of the area where sonar activities operate (Scales et al. 2017), but uncertainty on the boundaries of such area also presents an issue. Access to reliable information on the spatial and temporal patterns of sonar occurrence is critical for the proposed approach. The comparison of the SPORTS database with acoustic recordings on Navy ranges has shown that the database is prone to transcription errors and incomplete records (Falcone et al. 2017), which have likely contributed to the problems encountered when fitting the model to the additional case studies.

Beyond the effects of disturbance resulting from military sonar operations on cetacean species, our approach can be used to quantify the exposure to any activity that occurs within a discrete area and has either an attractive or a repulsive effect on exposed animals. Potential examples include attendance of marine predators to fish farms (Callier et al. 2018), changes in use of wind farm areas by birds (Pearce-Higgins et al. 2009), attractions to supplemental feeding sites for a range of species (Corcoran et al. 2013), temporal variation in the use of refuges as a function of anthropogenic risk in terrestrial ungulates (Visscher et al. 2017), or elephant occurrence in areas with differential human-associated mortality risk (Graham et al. 2009). More generally, it is often valuable to assess the probability of occurrence within predefined regions, e.g., to evaluate the effectiveness of the boundaries of a protected area for covering the occupancy of a sufficiently large proportion of a population (Cabeza et al. 2004, Licona et al. 2011, Lea et al. 2016), a common application of telemetry data (Hays et al. 2019). The transition rates estimated in our model would inform decisions regarding such boundaries.

The approach can be easily extended to model additional states, that is, additional discrete areas where individual patterns of occurrence are of interest. For example, the model could be used to estimate the connectivity among multiple protected areas, or the degree of usage of distinct portions of a population's range (Webster et al. 2002, Espinoza et al. 2015). The effect of other covariates (e.g., environmental characteristics) on the transitions among areas could be included to elucidate the ecological or anthropogenic processes influencing these movement patterns (Hanks et al. 2015, Buderman et al. 2018).

In conclusion, we introduced a versatile method to monitor animals' attendance to discrete areas in continuous time, and assess the effects of stressors or attractors on the transition rates across these predefined

boundaries. We used the method to quantify the effect of sonar on the occurrence of a cetacean species on a U.S. Navy range, and found changes in the propensity of moving in to and out of this area as a result of exposure. These results will help to assess the aggregate exposure of individuals and any resulting population-level consequences. However, we anticipate the model could have wide applications in both applied and fundamental ecological studies that use telemetry data to characterize animal movements.

#### ACKNOWLEDGMENTS

This study was supported by Office of Naval Research (ONR) grant N00014-16-1-2858: “PCoD+: Developing widely applicable models of the population consequences of disturbance”. We thank Ruth Joy, Rob Schick, John Harwood, Cormac Booth, Leslie New, Dan Costa, and Lisa Schwarz for useful discussions. Tagging in AUTEK was conducted under Bahamas Marine Mammal Research Permit #12A, issued by the Government of the Bahamas to the Bahamas Marine Mammal Research Organization (BMMRO) under the regulatory framework of the Bahamas Marine Mammal Protection Act (2005). Methods of deployment, tag types, and sample sizes were preapproved by BMMRO’s Institutional Animal Care and Use Committee (IACUC) and by the U.S. Department of the Navy, Bureau of Medicine and Surgery Veterinary Affairs Office. Protocols were reviewed annually by BMMRO’s IACUC throughout the duration of the study. Funding support for tagging was provided by the U.S. Navy’s ONR and Living Marine Resources (LMR) program, the Chief of Naval Operations’ Energy and Environmental Readiness Division and the NOAA Fisheries Ocean Acoustics Program (see Joyce et al. [2020] for details). We thank Charlotte Dunn, Leigh Hickmott, Holly Fearnbach, and the Marine Mammal Monitoring on Navy Ranges acoustic team at the U.S. Naval Undersea Warfare Center for support during fieldwork. Hawai’i tagging research was undertaken under NMFS Scientific Research Permits No. 731-1774 and 15330. Hawai’i field efforts were funded by the U.S. Navy (Pacific Fleet, LMR) and the National Marine Fisheries Service (Pacific Islands Fisheries Science Center). In SOCAL, tags were deployed under U.S. National Marine Fisheries Service permit numbers 540-1811 and 16111. All tags, in Hawai’i and SOCAL, were deployed in accordance with the IACUC guidelines for satellite tagging established by Cascadia Research Collective. Field efforts were supported by grants from the U.S. Navy’s LMR and N45 programs. The authors wish to acknowledge the use of New Zealand eScience Infrastructure (NeSI) high performance computing facilities as part of this research (<https://www.nesi.org.nz>). Finally, we thank the two anonymous reviewers and editor for their helpful comments and suggestions, which were greatly appreciated. C. Jones-Todd, E. Pirotta, and L. Thomas conceived the ideas and developed the methodology; R. W. Baird, J. Durban, E. Falcone, D. E. Claridge, G. Schorr, and S. Watwood collected and obtained permissions for use of the data. C. Jones-Todd and E. Pirotta analyzed the data and led the writing of the manuscript. All authors contributed critically to the drafts and gave final approval for publication. C. Jones-Todd and E. Pirotta contributed equally to this paper.

#### LITERATURE CITED

- Aguirre-Hernández, R., and V. Farewell. 2002. A Pearson-type goodness-of-fit test for stationary and time-continuous Markov regression models. *Statistics in Medicine* 21:1899–1911.
- Albertsen, C. M. 2017. argosTrack: fit movement models to Argos data for marine animals. R Package Version 1.1.0. <https://github.com/calbertsen/argosTrack>
- Albertsen, C. M., K. Whoriskey, D. Yurkowski, A. Nielsen, and J. Mills. 2015. Fast fitting of non-Gaussian state-space models to animal movement data via Template Model Builder. *Ecology* 96:2598–2604.
- Baird, R. W. 2016. *The lives of Hawai’i’s dolphins and whales: natural history and conservation*. University of Hawai’i Press, Honolulu, Hawai’i, USA.
- Baird, R. W., et al. 2019. Odontocete studies on the Pacific Missile Range Facility in August 2018: satellite-tagging, photo-identification, and passive acoustic monitoring. Prepared for Commander, Pacific Fleet, under Contract No. N62470-15-D-8006 Task Order 6274218F0107 issued to HDR Inc., Honolulu, Hawai’i, USA.
- Bejder, L., A. Samuels, H. Whitehead, and N. Gales. 2006. Interpreting short-term behavioural responses to disturbance within a longitudinal perspective. *Animal Behaviour* 72:1149–1158.
- Bernaldo de Quirós, Y., et al. 2019. Advances in research on the impacts of anti-submarine sonar on beaked whales. *Proceedings of the Royal Society B* 286:20182533.
- Bolker, B. M., M. E. Brooks, C. J. Clark, S. W. Geange, J. R. Poulsen, M. H. H. Stevens, and J. S. S. White. 2009. Generalized linear mixed models: a practical guide for ecology and evolution. *Trends in Ecology and Evolution* 24:127–135.
- Buderman, F. E., M. B. Hooten, M. W. Alldredge, E. M. Hanks, and J. S. Ivan. 2018. Time-varying predatory behavior is primary predictor of fine-scale movement of wildland-urban cougars. *Movement Ecology* 6:22.
- Cabeza, M., M. B. Araújo, R. J. Wilson, C. D. Thomas, M. J. R. Cowley, and A. Moilanen. 2004. Combining probabilities of occurrence with spatial reserve design. *Journal of Applied Ecology* 41:252–262.
- Callier, M. D., et al. 2018. Attraction and repulsion of mobile wild organisms to finfish and shellfish aquaculture: a review. *Reviews in Aquaculture* 10:924–949.
- Carter, M. I., B. T. McClintock, C. B. Embling, K. A. Bennett, D. Thompson, and D. J. Russell. 2020. From pup to predator: generalized hidden Markov models reveal rapid development of movement strategies in a naïve long-lived vertebrate. *Oikos* 129:630–642.
- Chaise, L. L., I. Prinet, C. Toscani, S. L. Gallon, W. Paterson, D. J. McCafferty, M. Thèry, A. Ancel, and C. Gilbert. 2018. Local weather and body condition influence habitat use and movements on land of molting female southern elephant seals (*Mirounga leonina*). *Ecology and Evolution* 8:6081–6090.
- Corcoran, M. J., B. M. Wetherbee, M. S. Shivji, M. D. Potenski, D. D. Chapman, and G. M. Harvey. 2013. Supplemental feeding for ecotourism reverses diel activity and alters movement patterns and spatial distribution of the southern stingray, *Dasyatis Americana*. *PLoS One* 8:e59235.
- Costa, D. P., et al. 2010. Accuracy of ARGOS locations of pinnipeds at-sea estimated using fastloc GPS. *PLoS One* 5:e8677.
- De-Ruiter, S. L., et al. 2013. First direct measurements of behavioural responses by Cuvier’s beaked whales to mid-frequency active sonar. *Biology Letters* 9:20130223.
- De-Ruiter, S. L., R. Langrock, T. Skirbutas, J. A. Goldbogen, J. Calambokidis, A. S. Friedlaender, and B. L. Southall. 2017. A multivariate mixed hidden Markov model for blue whale behaviour and responses to sound exposure. *Annals of Applied Statistics* 11:362–392.
- Diaz, S., et al. 2019. Summary for policymakers of the global assessment report on biodiversity and ecosystem services of the intergovernmental science-policy platform on biodiversity

- and ecosystem services. Intergovernmental Science-Policy Platform on Biodiversity and Ecosystem Services (IPBES). <https://uwe-repository.worktribe.com/output/1493508>
- Donovan, C. R., C. M. Harris, L. Milazzo, J. Harwood, L. Marshall, and R. Williams. 2017. A simulation approach to assessing environmental risk of sound exposure to marine mammals. *Ecology and Evolution* 7:2101–2111.
- Ersts, P. J., and H. C. Rosenbaum. 2003. Habitat preference reflects social organization of humpback whales (*Megaptera novaeangliae*) on a wintering ground. *Journal of Zoology* 260:337–345.
- Espinoza, M., E. J. I. Lédée, C. A. Simpfendorfer, A. J. Tobin, and M. R. Heupel. 2015. Contrasting movements and connectivity of reef-associated sharks using acoustic telemetry: implications for management. *Ecological Applications* 25:2101–2118.
- Falcone, E. A., G. S. Schorr, S. L. Watwood, S. L. De Ruiter, A. N. Zerbini, R. D. Andrews, R. P. Morrissey, and D. J. Moretti. 2017. Diving behaviour of Cuvier's beaked whales exposed to two types of military sonar. *Royal Society Open Science* 4: 170629.
- Frankel, A. S., W. T. Ellison, and J. Buchanan. 2002. Application of the Acoustic Integration Model (AIM) to predict and minimize environmental impacts. *IEEE Journal of Oceanic Engineering* 3:1438–1443.
- Freitas, C. 2012. argosfilter: Argos locations filter. R package version 0.63. <https://github.com/cran/argosfilter>
- Frid, A., and L. M. Dill. 2002. Human-caused disturbance stimuli as a form of predation risk. *Conservation Ecology* 6:11.
- Graham, M. D., I. Douglas-Hamilton, W. M. Adams, and P. C. Lee. 2009. The movement of African elephants in a human-dominated land-use mosaic. *Animal Conservation* 12:445–455.
- Halpern, B. S., et al. 2008. A global map of human impact on marine ecosystems. *Science* 319:948–952.
- Hanks, E. M., M. B. Hooten, and M. W. Allredge. 2015. Continuous-time discrete-space models for animal movement. *Annals of Applied Statistics* 9:145–165.
- Harris, C. M., et al. 2018. Marine mammals and sonar: dose-response studies, the risk-disturbance hypothesis and the role of exposure context. *Journal of Applied Ecology* 55:396–404.
- Hauser, D. D., M. G. Logsdon, E. E. Holmes, G. R. VanBlaricom, and R. W. Osborne. 2007. Summer distribution patterns of southern resident killer whales *Orcinus orca*: core areas and spatial segregation of social groups. *Marine Ecology Progress Series* 351:301–310.
- Hays, G. C., et al. 2019. Translating marine animal tracking data into conservation policy and management. *Trends in Ecology and Evolution* 34:459–473.
- Hewitt, J., R. S. Schick, and A. E. Gelfand. 2021. Continuous-time discrete-state modeling for deep whale dives. *Journal of Agricultural, Biological and Environmental Statistics* 26:180–199.
- Hooten, M. B., F. E. Buderman, B. M. Brost, E. M. Hanks, and J. S. Ivan. 2016. Hierarchical animal movement models for population-level inference. *Environmetrics* 27:322–333.
- Houser, D. S. 2006. A method for modeling marine mammal movement and behavior for environmental impact assessment. *IEEE Journal of Oceanic Engineering* 31:76–81.
- Hückstädt, L. A., L. K. Schwarz, A. S. Friedlaender, B. R. Mate, A. N. Zerbini, A. Kennedy, J. Robbins, N. J. Gales, and D. P. Costa. 2020. A dynamic approach to estimate the probability of exposure of marine predators to oil exploration seismic surveys over continental shelf waters. *Endangered Species Research* 42:185–199.
- Jackson, C. H. 2011. Multi-state models for panel data: The msm package for R. *Journal of Statistical Software* 38:1–29.
- Johnson, D. S., J. M. London, M.-A. Lea, and J. W. Durban. 2008. Continuous-time correlated random walk model for animal telemetry data. *Ecology* 89:1208–1215.
- Jones, E. L., G. D. Hastie, S. Smout, J. Onoufriou, N. D. Merchant, K. L. Brookes, and D. Thompson. 2017. Seals and shipping: quantifying population risk and individual exposure to vessel noise. *Journal of Applied Ecology* 54:1930–1940.
- Jones-Todd, C. M. 2021. cmjt/mmmre: Release for accepted manuscript. Zenodo. <https://doi.org/10.5281/zenodo.4876540>
- Jones-Todd, C. M., E. Pirodda, J. Durban, D. Claridge, R. W. Baird, E. Falcone, G. Schorr, S. Watwood, and L. Thomas. 2021. Discrete-space continuous-time models of marine mammal exposure to Navy sonar (Version 3). *Dryad*. <https://doi.org/10.5061/DRYAD.DR7SQV9ZB>
- Joyce, T. W., J. W. Durban, D. E. Claridge, C. A. Dunn, L. S. Hickmott, H. Fearnbach, K. Dolan, and D. Moretti. 2020. Behavioral responses of satellite tracked Blainville's beaked whales (*Mesoplodon densirostris*) to mid-frequency active sonar. *Marine Mammal Science* 36:29–46.
- Kristensen, K., A. Nielsen, C. W. Berg, H. Skaug, and B. M. Bell. 2016. TMB: Automatic differentiation and Laplace approximation. *Journal of Statistical Software* 70:1–21.
- Langrock, R., R. King, J. Matthiopoulos, L. Thomas, D. Fortin, and J. M. Morales. 2012. Flexible and practical modeling of animal telemetry data: hidden Markov models and extensions. *Ecology* 93:2336–2342.
- Lea, J. S. E., N. E. Humphries, R. G. von Brandis, C. R. Clarke, and D. W. Sims. 2016. Acoustic telemetry and network analysis reveal the space use of multiple reef predators and enhance marine protected area design. *Proceedings of the Royal Society B* 283:20160717.
- Licona, M., R. McCleery, B. Collier, D. J. Brightsmith, and R. Lopez. 2011. Using ungulate occurrence to evaluate community-based conservation within a biosphere reserve model. *Animal Conservation* 14:206–214.
- Lopez, R., J.-P. Malarde, F. Royer, and P. Gaspar. 2013. Improving argos doppler location using multiple-model Kalman filtering. *IEEE Transactions on Geoscience and Remote Sensing* 52:4744–4755.
- Manzano-Roth, R., E. E. Henderson, S. W. Martin, C. Martin, and B. M. Matsuyama. 2016. Impacts of U.S. Navy training events on Blainville's beaked whale (*Mesoplodon densirostris*) foraging dives in Hawaiian waters. *Aquatic Mammals* 42:507.
- McCarthy, E., D. Moretti, L. Thomas, N. DiMarzio, R. Morrissey, S. Jarvis, J. Ward, A. Izzi, and A. Dilley. 2011. Changes in spatial and temporal distribution and vocal behavior of Blainville's beaked whales (*Mesoplodon densirostris*) during multiship exercises with mid-frequency sonar. *Marine Mammal Science* 27:E206–E226.
- McClintock, B. T. 2017. Incorporating telemetry error into hidden Markov models of animal movement using multiple imputation. *Journal of Agricultural, Biological and Environmental Statistics* 22:249–269.
- Montgomery, J. C., and C. A. Radford. 2017. Marine bioacoustics. *Current Biology* 27:R502–R507.
- Moretti, D., et al. 2014. A risk function for behavioral disruption of Blainville's beaked whales (*Mesoplodon densirostris*) from mid-frequency active sonar. *PLoS One* 9:e85064.
- National Research Council. 2005. Marine mammal populations and ocean noise: determining when noise causes biologically significant effects. National Academies Press, Washington, D.C., USA.
- Nowacek, D. P., L. H. Thorne, D. W. Johnston, and P. L. Tyack. 2007. Responses of cetaceans to anthropogenic noise. *Mammal Review* 37:81–115.
- Pack, A. A., L. M. Herman, A. S. Craig, S. S. Spitz, J. O. Waterman, E. Y. K. Herman, M. H. Deakos, S. Hakala, and

- C. Lowe. 2017. Habitat preferences by individual humpback whale mothers in the Hawaiian breeding grounds vary with the age and size of their calves. *Animal Behaviour* 133:131–144.
- Patterson, T. A., B. J. McConnell, M. A. Fedak, M. V. Bravington, and M. A. Hindell. 2010. Using GPS data to evaluate the accuracy of state space methods for correction of Argos satellite telemetry error. *Ecology* 91:273–285.
- Patterson, T. A., A. Parton, R. Langrock, P. G. Blackwell, L. Thomas, and R. King. 2017. Statistical modelling of individual animal movement: an overview of key methods and a discussion of practical challenges. *ASTA Advances in Statistical Analysis* 101:399–438.
- Pearce-Higgins, J. W., L. Stephen, R. H. Langston, I. P. Bainbridge, and R. Bullman. 2009. The distribution of breeding birds around upland wind farms. *Journal of Applied Ecology* 46:1323–1331.
- Pirotta, E., et al. 2018a. Understanding the population consequences of disturbance. *Ecology and Evolution* 8:9934–9946.
- Pirotta, E., L. New, and M. Marcoux. 2018b. Modelling beluga habitat use and baseline exposure to shipping traffic to design effective protection against prospective industrialization in the Canadian Arctic. *Aquatic Conservation: Marine and Freshwater Ecosystems* 28:713–722.
- Popper, A. N., and A. Hawkins. 2016. *The effects of noise on aquatic life II*. Springer, New York, New York, USA.
- Sanderson, E. W., M. Jaiteh, M. A. Levy, K. H. Redford, A. V. Wannebo, and G. Woolmer. 2002. The human footprint and the last of the wild: the human footprint is a global map of human influence on the land surface, which suggests that human beings are stewards of nature, whether we like it or not. *BioScience* 52:891–904.
- Scales, K. L., G. S. Schorr, E. L. Hazen, S. J. Bograd, P. I. Miller, R. D. Andrews, A. N. Zerbini, and E. A. Falcone. 2017. Should I stay or should I go? Modelling year-round habitat suitability and drivers of residency for fin whales in the California Current. *Diversity and Distributions* 23:1204–1215.
- Scharf, H., M. B. Hooten, B. K. Fosdick, D. S. Johnson, J. M. London, and J. W. Durban. 2016. Dynamic social networks based on movement. *Annals of Applied Statistics* 10:2182–2202.
- Scharf, H., M. B. Hooten, and D. S. Johnson. 2017. Imputation approaches for animal movement modeling. *Journal of Agricultural, Biological and Environmental Statistics* 22:335–352.
- Southall, B. L., D. P. Nowacek, P. J. Miller, and P. L. Tyack. 2016. Experimental field studies to measure behavioral responses of cetaceans to sonar. *Endangered Species Research* 31:293–315.
- Stewart, B. S. 1997. Ontogeny of differential migration and sexual segregation in northern elephant seals. *Journal of Mammalogy* 78:1101–1116.
- Stimpert, A. K., S. L. De Ruiter, B. L. Southall, D. J. Moretti, E. A. Falcone, J. A. Goldbogen, A. Friedlaender, G. S. Schorr, and J. Calambokidis. 2014. Acoustic and foraging behavior of a Baird's beaked whale, *Berardius bairdii*, exposed to simulated sonar. *Scientific Reports* 4:7031.
- Tyack, P. L., et al. 2011. Beaked whales respond to simulated and actual navy sonar. *PLoS One* 6:e17009.
- U.S. Department of the Navy. 2018. Quantifying acoustic impacts on marine mammals and sea turtles: methods and analytical approach for phase iii training and testing. Technical Report. NUWC Division Newport, Space and Naval Warfare Systems Center Pacific, G2 Software Systems, and the National Marine Mammal Foundation, Naval Undersea Warfare Center, Newport, Rhode Island, USA.
- Vaida, F., and S. Blanchard. 2005. Conditional Akaike information for mixed-effects models. *Biometrika* 92:351–370.
- Visscher, D. R., I. Macleod, K. Vujnovic, D. Vujnovic, and P. D. Dewitt. 2017. Human risk induced behavioral shifts in refuge use by elk in an agricultural matrix. *Wildlife Society Bulletin* 41:162–169.
- Webster, M. S., P. P. Marra, S. M. Haig, S. Bensch, and R. T. Holmes. 2002. Links between worlds: unraveling migratory connectivity. *Trends in Ecology & Evolution* 17:76–83.
- Wensveen, P. J., et al. 2019. Northern bottlenose whales in a pristine environment respond strongly to close and distant navy sonar signals. *Proceedings of the Royal Society B* 286:20182592.

#### SUPPORTING INFORMATION

Additional supporting information may be found online at: <http://onlinelibrary.wiley.com/doi/10.1002/eap.2475/full>

#### OPEN RESEARCH

Code and example data are available in the R package `mmre` (Jones-Todd 2021), see <https://doi.org/10.5281/zenodo.4876540> and Appendix S3. Raw Argos whale tracking data are available from the Dryad Digital Repository, <https://doi.org/10.5061/dryad.dr7sqv9zb> (Jones-Todd et al. 2021). The sonar data supporting this research are not accessible to the public, but are available from the Naval Undersea Warfare Center. To gain access please contact the Naval Undersea Warfare Center Division directly, <https://www.navsea.navy.mil/Home/Warfare-Centers/NUWC-Newport/Contact-U/>